

9<sup>th</sup> International Conference on Photonic Technologies - LANE 2016

## Laser metal deposition as repair technology for a gas turbine burner made of Inconel 718

Torsten Petrat<sup>a,\*</sup>, Benjamin Graf<sup>a</sup>, Andrey Gumenyuk<sup>a,b</sup>, Michael Rethmeier<sup>a,b,c</sup>

<sup>a</sup>Fraunhofer Institut for Production Systems and Design Technology, Pascalstraße 8-9, 10587 Berlin, Germany

<sup>b</sup>Federal Institute for Materials Research and Testing, Unter den Eichen 87, 12205 Berlin, Germany

<sup>c</sup>Technical University Berlin, Institute of Machine Tools and Factory Management, Pascalstraße 8-9, 10587 Berlin, Germany

---

### Abstract

Maintenance, repair and overhaul of components are of increasing interest for parts of high complexity and expensive manufacturing costs. In this paper a production process for laser metal deposition is presented, and used to repair a gas turbine burner of Inconel 718. Different parameters for defined track geometries were determined to attain a near net shape deposition with consistent build-up rate for changing wall thicknesses over the manufacturing process. Spot diameter, powder feed rate, welding velocity and laser power were changed as main parameters for a different track size. An optimal overlap rate for a constant layer height was used to calculate the best track size for a fitting layer width similar to the part dimension. Deviations in width and height over the whole build-up process were detected and customized build-up strategies for the 3D sequences were designed. The results show the possibility of a near net shape repair by using different track geometries with laser metal deposition.

© 2016 The Authors. Published by Elsevier B.V. This is an open access article under the CC BY-NC-ND license (<http://creativecommons.org/licenses/by-nc-nd/4.0/>).

Peer-review under responsibility of the Bayerisches Laserzentrum GmbH

**Keywords:** Laser metal deposition; Inconel 718; additive manufacturing; maintenance, repair and overhaul

---

### 1. Introduction

Additive technologies are getting more and more attention in the area of development as well as in production. Light weight structures, integrated functions and fast design changes in the production are of high interest. A rising trust into the processes makes a step from prototyping to the manufacturing possible, which is shown by Wohler

---

\* Corresponding author. Tel.: +49-30-39006-375 ; fax: +49-30-39006-391 .

E-mail address: [Torsten.petrat@ipk.fraunhofer.de](mailto:Torsten.petrat@ipk.fraunhofer.de)

(2011) in a higher number of sold machines. The engineers have to learn and use the possibility of a new freedom by designing adapted parts for special applications, Vayre et al. (2012). Prototypes as well as serial parts can be built on the same machine and design changes are implemented in the next production cycle. These things make the technologies predestined for small batch sizes. Challenges are the long cycles to validate new forms and materials. In the future the production has to be first-time-right for a better acceptance.

Laser metal deposition (LMD) is among the additive technologies. A powder nozzle in combination with a laser beam is used to build 3D components consisting of single weld tracks. The laser beam creates a melting pool on the surface of the part. The filler material is injected by a nozzle and melts as well. The solidification results in a metallurgical bonding to the base material. The powder is carried by an inert gas like helium and the treatment area is typically shielded by argon. The key process parameters are the laser power, welding velocity, powder mass flow and beam spot diameter. By them the height and width of single tracks can be influenced, which is shown for co-axial, Graf et al. (2013) and off-axial, Ocelik et al. (2007) nozzles. An increase of temperature over the building process leads to an increase of the melt pool and creates a bigger track width. Cooling times between the layers and a laser power adjustment can control the melt pool width, Graf et al. (2015) and Ocylok et al. (2014). The process is shown in Fig. 1. Single tracks can be placed next to each other to create a layer. By stacking the layers it is possible to fabricate 3D parts. The use of a small track size allows a higher accuracy of the resulting component. The general smaller build-up rate increases the processing time. A combination of different track sizes in one part shows high accuracy as well as high building speed, Petrat et al. (2015).

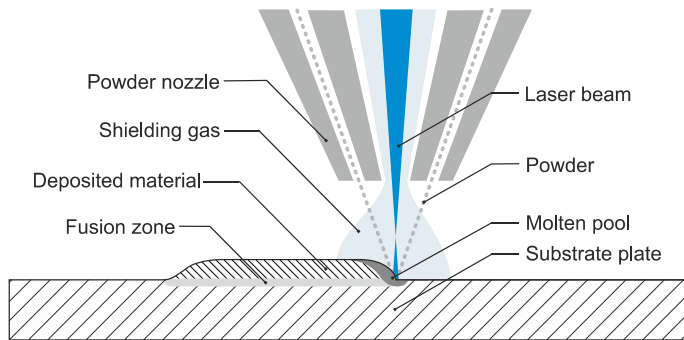


Fig. 1. (a) Layer composition; (b) layer traverse.

Advantages of the technology are precise depositions, graded material use and a low heat input, which results in a low distortion and a small heat affected zone. The weld pool has a small size and minimizes the dilution of base and filler material down to 5%. Scopes of application are repair of expensive parts like turbine blades or die tools, coatings for wear protection and fast prototyping of new parts in development. In relation to a low carbon footprint it is shown, that a damaged part volume of less than 18% is necessary compared to replace it by a new manufactured blade. Higher laser efficiency as well as increasing complexity of turbine components influence the carbon footprint and may change this value. The resulting mechanical properties of a remanufactured turbine blade of nickel-base alloys are comparable to standard components, Wilson et al. (2014). A process-orientated preparation is necessary to avoid bonding defects and ensure an unaffected process, Graf et al. (2012).

For thin walls consisting of single tracks a controlled LMD process is presented by Guijun and Gasser (2011). Increasing temperatures over the building time influence the melt pool and lead to an excessive build-up in corner areas and an inclination of the sidewall. A regulation of the laser power relating to the melt pool temperature avoids the irregularities.

The overlap range of the aligned tracks influences the geometry of the surface. A constant height from first to last track of a layer is given by an overlap ratio of near 30%, Li et al. (1997) and Nenadi et al. (2014). Higher rates add up over the first tracks before a constant layer height occurs. Different strategies have an influence on the accuracy of dimension and shape of single layers as well as over the whole build-up process. Peripheral areas have a lower deposition by using a nozzle orientation perpendicular to the surface of a specimen. It was studied that compensation

is possible by an inclination of the powder nozzle, Hensinger et al. (2000). That requires free space for the tool movement. A perpendicular orientation can also be compensated by additional superimposed tracks, Petrat et al. (2015). A contour layer combined with a customized pendulum strategy avoids the stair-step effect by cylindrical shapes. Pendulum strategies are showing better results of defects and material bonding compared to decreasing contour or spiral strategies, Calleja et al. (2014).

## 2. Experimental

### 2.1. Materials and experimental procedure

The experiments were conducted with a TRUMPF TruDisk 2.0 kW Yb:YAG laser and a 3-jet powder nozzle. The setup of the carrier gas Helium 5.0 with 4 l/min and the shielding gas Argon 5.0 with 10 l/min were constant for all experiments. The powder material with a grain size of 45  $\mu\text{m}$  to 90  $\mu\text{m}$  as well as the ground materials consisted of the nickel-base alloy Inconel 718. The chemical composition of the powder is shown in Table 1.

Table 1. Chemical composition of Inconel 718, manufacturer specification in wt-%.

Cr	Mo	Al	Cu	Nb	Ti	Fe	C	Ni
19.05	3.10	0.48	0.02	5.16	0.96	18.18	0.05	balance

The orientation of the powder nozzle is in all experiments perpendicular to the top surface of the component. The overlap ratio for the layers is  $30\% \pm 3\%$ .

### 2.2. Component shape and build-up strategies

The connection area of a gas turbine burner manufactured by selective laser melting (SLM) was removed for a rebuild with LMD. The shape of the repairing part of the component corresponds to a hollow cylinder with three different sizes of height, wall thickness and diameter over the whole build direction. Five parameter sets were used for the build-up investigations, Table 2.

Table 2. Used parameter sets.

Parameter	DoE space	PS 1	PS 2	PS 3	PS 4	PS 5
Laser power in W	800 to 1600	800	800	800	800	1200
Spot diameter in mm	1.0 to 2.2	1.0	1.0	1.6	1.6	2.2
Welding velocity in mm/min	600 to 1000	800	1000	600	800	600
Powder mass flow in g/min	5 to 15	10	15	10	10	15

The component was sliced into three single hollow cylinders C1, C2 and C3. Table 3 shows the wall thicknesses of the cylinders. A pool of different track sizes is given by previous studies using a DoE, which parameter space is shown in Table 2. The parameter sets with the best weld penetration and surface roughness were chosen. The best fitting tracks are identified by a calculation for a near net shape and an overlap ratio close to 30%. An oversize up to 0.8 mm was used.

Table 3. Wall thickness of different parts.

Part	Wall thickness	Oversize of 0 mm		Oversize of 0.3 mm		Oversize of 0.8 mm	
	in mm	Parameter set	Overlap ratio	Parameter set	Overlap ratio	Parameter set	Overlap ratio
C1	7.5	PS 1	30.5 %	PS 3	29.8 %	PS 2	30.0 %
C2	3	PS 3	27.2 %	PS 2	32.7 %	PS 4	28.5 %
C3	2	-	-	PS 5	-	-	-

A single layer was built by circles of different diameter. The starting point was changed along the contour after each layer by  $25^\circ$ . Three build-up strategies were investigated with different combinations of layer compositions. The layer compositions are shown in Fig. 2. The preliminary investigations of the single parts were made on substrate plates. Afterwards the combined build-up was transferred to rebuild the connection area of the gas turbine burner. The surfaces of the specimens were cleaned with acetone before the process.

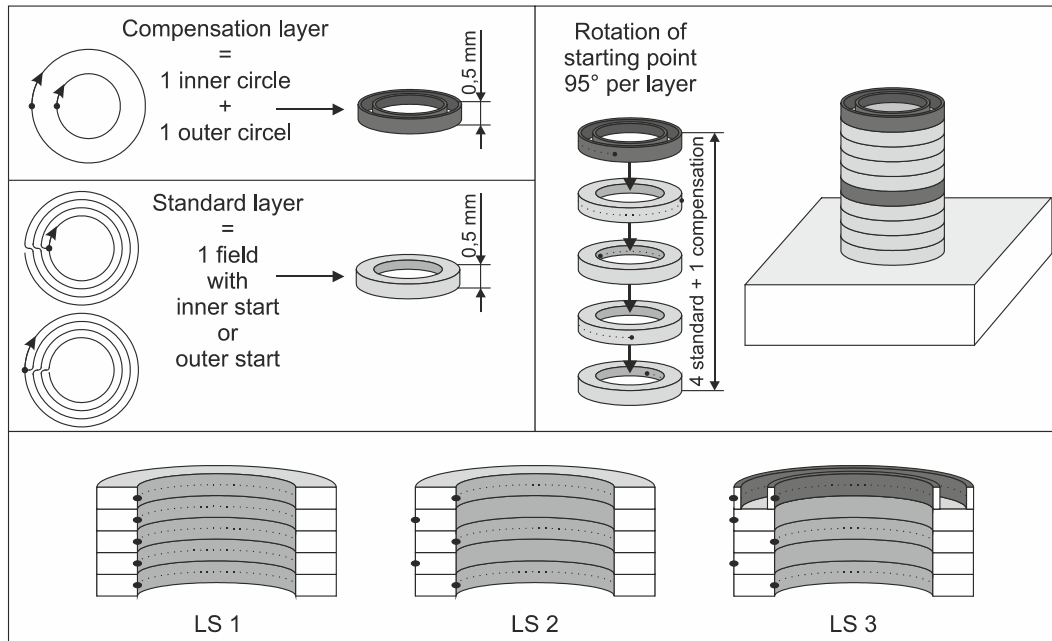


Fig. 2. (a) Layer composition; (b) layer traverse.

### 3. Results and Discussion

#### 3.1. Build up strategies and near net shape

The experimental results are schematically shown in Fig. 3. The starting point rotation along the edge avoids error propagation like it is mentioned by Zhang et al. (2003) for single walled tube parts and by Petrat et al. (2015) for full parts of cylindrical shape. The starting points are visible on the sidewall and after each layer, but do not add up over the process. Strategy LS 1 with a starting point on the same edge leads to a fall off in the inner area in contrast to the outer end area. This behavior is detected by the different parameter combinations and wall thicknesses. After four layers the inner edge has a lower height of more than one single track. This has a negative influence on the following build-up, which can be seen by weld beads. The fall off spreads over to track two and three within the following layers. A small decrease is also detected on the edge of the end area.

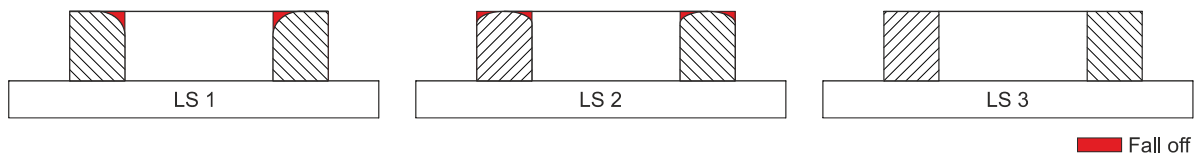


Fig. 3. Build-up of different strategies.

The changing start edge in LS 2 delays the fall off and equalizes the inner and outer edge area. Two to three additional outer circles are needed after 10 layers to balance the height.

An additional outer and inner circle every 4 layers are used in strategy LS 3. A hollow cylinder C1 with strategy LS 1 and LS 3 is shown in Fig. 4. The edge areas are equal to the inner field and the build-up is constant over 12 layers.

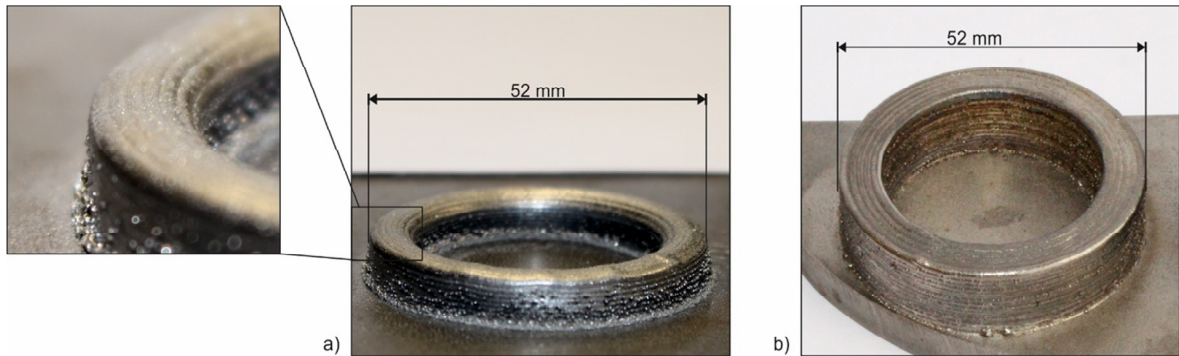


Fig. 4. Hollow cylinder with (a) strategy LS 1 and (b) strategy LS 3.

The measured wall thicknesses of the build-up strategies can be seen in Table 4 after a different number of layers. All strategies show a similar thickness in the first layers. LS 1 and LS 2 have a decrease in the following build-up process, which results in slopping side walls. The fall off by LS 1 leads to a deviation of more than 0.5 mm. The deviation of LS 2 is with 0.2 mm much smaller, but it is expected, that the increasing fall off will result in an increasing deviation. A constant build-up is achieved with strategy LS 3. The wall thickness varies between 7.20 mm and 7.34 mm. The higher values were measured in the area of the additional outer circles.

Table 4. Wall thickness with different build-up strategies and an oversize of 0 mm.

Strategy	LS 1	LS 2	LS 3
After 3 layers	7.26 mm	7.23 mm	7.26 mm
After 6 layers	7.10 mm	7.16 mm	7.29 mm
After 10 layers	6.73 mm	7.03 mm	7.22 mm

The wall thicknesses of part C1 are measured for strategy LS 3 with different over dimensions and are shown in Table 5. All three parameter sets result in a deviation between calculated and measured part dimension.

Table 5. Wall thickness with build-up strategy LS 3 and different oversize.

oversize	0 mm	0.3 mm	0.8 mm
After 3 layers	7.26 mm	7.36 mm	7.93 mm
After 6 layers	7.29 mm	7.35 mm	8.03 mm
After 10 layers	7.22 mm	7.39 mm	7.95 mm

The target thickness is 7.5 mm with an oversize of 0.15 mm on each side of the wall, which results in a total wall thickness of 7.8 mm. In this case the deviation is not consistent over the different parameters. C1 with parameter set PS 1 and a calculated oversize of 0 mm has a smaller dimension of 0.21 mm to 0.28 mm. The use of parameter set PS 3 (Table 2.) for an oversize of 0.3 mm differs by 0.41 to 0.45 mm of calculated to measured value. This results in an undersized dimension of 0.11 mm to 0.15 mm to the nominal dimension. The deviation of parameter set PS 2 for an oversize of 0.8 mm is located between the others with a value of 0.27 to 0.37 mm. The oversize is 0.43 mm to

0.53 mm and allows a subtractive post processing to nominal dimensions. The measured oversize in this case is 0.06 mm to big on each side. The sidewalls have a surface roughness of 0.10 mm with LS 3. Similar results in build-up and near net shape are detected for part C2. Fig. 5 shows all single parts in the final height on a substrate plate. The differences in deviation can be explained by the calculation of the component geometry as well as the different parameter sets. The theoretical wall thickness is calculated by the size of single tracks, which are welded on a metal plate. The weld pool formation in edge areas differs from that and influences the resulting deposition. The weld beads on the side walls are indicating the loss of material in this region. The welding velocity additionally changes the heat input and the amount of material per section.

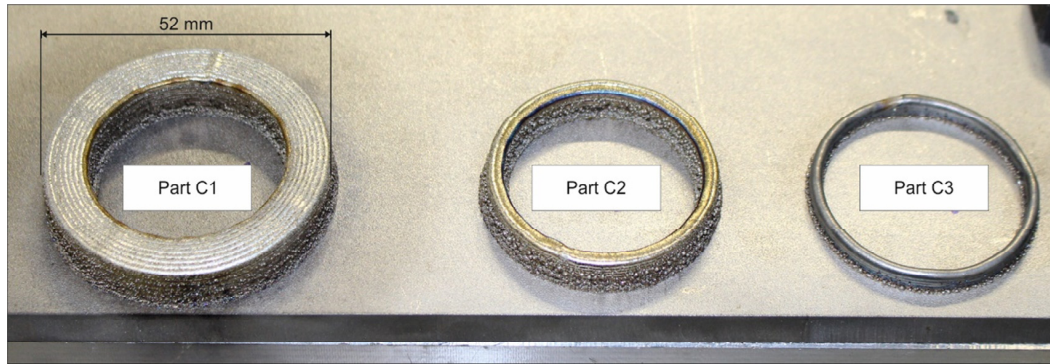


Fig. 5. Part C1, C2 and C3 in final height on a substrate plate.

### 3.2. Combined part repair

The combination of the single parts onto a substrate plate could be carried out without an adjustment of the investigated build-up strategies. The inner sidewall of a specimen with 10 layers of each part is shown in Fig. 6 a). The connection between the different parts is slightly seen in the area of the changing parameter sets and the small step between C2 and C3. The complete burner is shown in Fig. 6 b). The numbers of layers to achieve the final height of each part of the component are:

- 9 layers for C1
- 6 layers for C2
- 4 layers for C3

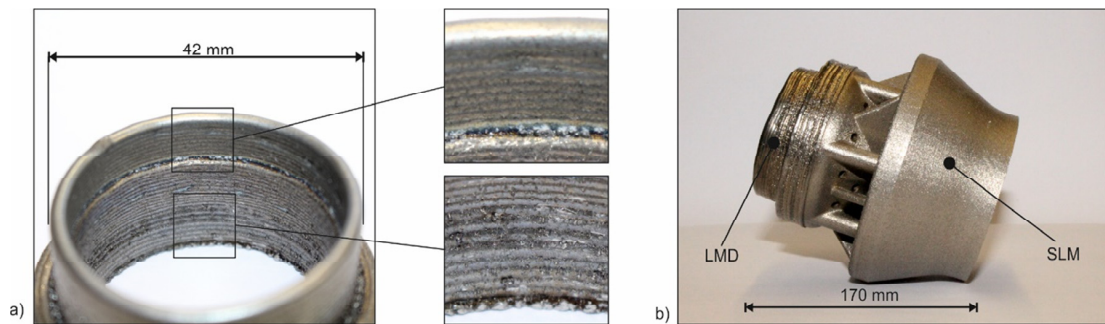


Fig. 6. (a) Inner sidewall of combined component and (b) complete burner rebuild.



An analysis of the microsection shows an undirected dendritic microstructure in all three parts C1, C2 and C3 of the component, Fig. 7. The different parameter sets indicate no influence on grain growth. Consequently, the choice of the parameters can be made on basis of the resulting track width, which allows a near net shape manufacturing without differences of the resulting structure.

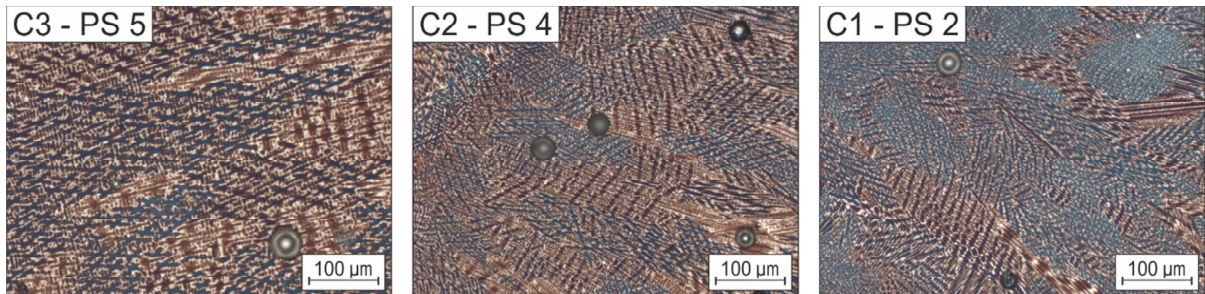


Fig. 7. Microstructure of the different parts C1, C2 and C3.

The porosity is analyzed by a phase-distribution with Imagic IMS Client of metallographic cross sections and shows up to 3% in the LMD build up. The highest number of pores is detected in the area of track and layer bonding especially for C1 and C2 with adjacent tracks for layer creation, Fig. 8. One reason might be a too low laser power, so the higher laser power of part C3 shows a bigger track size but a similar porosity like the other parts. The hardness of different LMD parts and parameters are consistent over the whole build-up, Fig. 8. A decrease of 50 HV1 to 100 HV1 is detected between the SLM generated ground material and the LMD part.

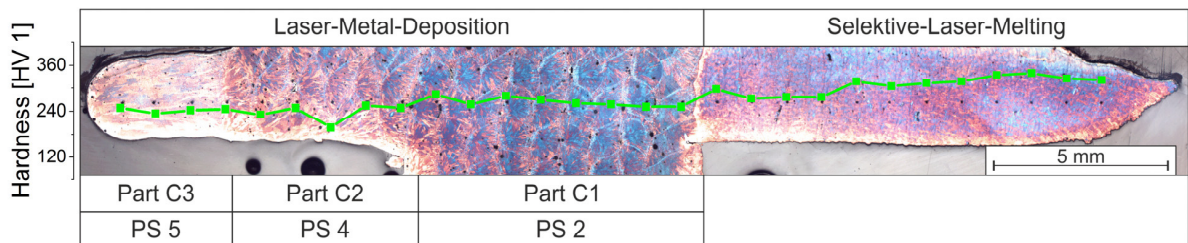


Fig. 8. Hardness over the build-up.

#### 4. Conclusion

The investigations show the possibility of different track sizes for a near net shape. Deviations were detected between calculated part sizes by using the measured width of single tracks. A down fall of edge areas can be compensated by adjusted build-up strategies. Changes of the starting point between inner and outer edge as well as additional tracks were needed for a constant component growth. A rebuild could be shown for the connection area of a turbine gas burner. The porosity is constant over the whole LMD part and no difference could be measured between a high and a low laser power.

#### Acknowledgements

The authors would like to acknowledge the Investitionsbank Berlin IBB for funding the research by their support program ProFit and the Federal Institute for Materials Research and Testing for support.

## References

- Bi, G., Gasser, A. 2011. Restoration of Nickel-Base Turbine Blade Knife-Edges with Controlled Laser Aided Additive Manufacturing. *Physics Procedia* 12(PART 1):402–9.
- Calleja, A., Tabernero, I., Fernández, A., Celaya, A., Lamikiz, A., López de Lacalle, L. N. 2014. Improvement of Strategies and Parameters for Multi-Axis Laser Cladding Operations. *Optics and Lasers in Engineering* 56:113–20.
- Graf, B., Ammer, S., Gumenyuk, A., Rethmeier, M. 2013. Design of Experiments for Laser Metal Deposition in Maintenance, Repair and Overhaul Applications. *Procedia CIRP* 11:245–48.
- Graf, B., Gumenyuk, A., Rethmeier, M. 2012. Laser Metal Deposition as Repair Technology for Stainless Steel and Titanium Alloys. *Physics Procedia* 39:376–81.
- Graf, B., Schuch, M., Kersting, R., Gumenyuk, A., Rethmeier, M. 2015. “Additive Process Chain Using Selective Laser Melting and Laser Metal Deposition.” *Lasers in Manufacturing Conference* 2015.
- Hensinger, D. M., Ames, A. L., Kuhlmann, J. L. 2000. Motion Planning for a Direct Metal Deposition Rapid Prototyping System. Pp. 3095–3100 in *Proceedings 2000 ICRA. Millennium Conference. IEEE International Conference on Robotics and Automation. Symposia Proceedings* (Cat. No.00CH37065), vol. 4. San Francisco: IEEE.
- Li, Y., Ma, J. 1997. Study on Overlapping in the Laser Cladding Process. *Surface and Coatings Technology* 90:1–5.
- Nenadl, O., Ocelik, V., Palavra, A., de Hosson, J. Th. M. 2014. The Prediction of Coating Geometry from Main Processing Parameters in Laser Cladding. *Physics Procedia* 56:220–27.
- Ocelik, V., de Oliveira, U., de Boer, M., de Hosson, J. Th. M. 2007. Thick Co-Based Coating on Cast Iron by Side Laser Cladding: Analysis of Processing Conditions and Coating Properties. *Surface and Coatings Technology* 201(12):5875–83.
- Ocylok, S., Alexeev, E., Mann, S., Weisheit, A., Wissenbach, K., Kelbassa, I. 2014. Correlations of Melt Pool Geometry and Process Parameters During Laser Metal Deposition by Coaxial Process Monitoring. *Physics Procedia* 56:228–38.
- Petrat, T., Graf, B., Gumenyuk, A., Rethmeier, M. 2015. Build-up Strategies for Generating Components of Cylindrical Shape with Laser Metal Deposition. *Lasers in Manufacturing Conference* 2015.
- Petrat, T., Graf, B., Gumenyuk, A., Rethmeier, M. 2015. Laser-Pulver-Auftragschweißen zum additiven Aufbau komplexer Formen. *DVS Congress* 2015 315:126–29.
- Vayre, B., Vignat, F., Villeneuve, F. 2012. Designing for Additive Manufacturing. *Procedia CIRP* 3:632–37.
- Wilson, J. M., Piya, C., Shin, Y. C., Zhao, F., Ramani, K. 2014. “Remanufacturing of Turbine Blades by Laser Direct Deposition with Its Energy and Environmental Impact Analysis.” *Journal of Cleaner Production* 80:170–78.
- Wohlers, T. 2011. *Additive Manufacturing and 3d Printing State of the Industry; Annual Worldwide Progress Report*. Fort Collins.